Short Communication

Limitations of Macroscopic Fluorescence Imaging for the Estimation of Tumour Growth in an Orthotopic Glioma Mouse Model

(*in vivo* fluorescence imaging / mKate2 / glioma growth)

M. HILŠER, J. TRYLČOVÁ, P. BUŠEK, A. ŠEDO

Institute of Biochemistry and Experimental Oncology, First Faculty of Medicine, Charles University in Prague, Czech Republic

Abstract. Imaging methods based on light detection are being increasingly used for the non-invasive assessment of tumour growth in animal models. In contrast with bioluminescence imaging, there are no studies assessing the use of macroscopic fluorescence imaging for the longitudinal monitoring of tumour growth in an orthotopic glioma mouse model. Glioma cells expressing the red-shifted fluorescent protein mKate2 were orthotopically implanted to NOD-rag mice and the tumour size estimated by macroscopic fluorescence imaging was compared to the tumour volume determined morphometrically. There was no significant correlation between the data obtained by non-invasive macroscopic fluorescence imaging and post mortem morphometry. In addition, the fluorescence imaging failed to detect a morphometrically verified difference in tumour volume between animals with tumours expressing a potential tumour suppressor gene and controls. The fluorescence signal was affected by the spatial pattern of tumour growth and substantially attenuated by the interfering brain tissue. Our results indicate that the fluorescence signal emitted by glioma cells reflected not only the tumour mass, but also its spatial distribution. Macroscopic planar FLI in an epi-illumination mode and a conventional source of excitation light therefore appears to be more suitable for semi-quantitative assessment of the tumour growth especially in the case of superficially located tumours rather than for precise volume estimation of the xenografts located deep within the brain tissue.

Introduction

The orthotopic brain tumour model is an important tool that has been applied in the research of brain malignancies for many years (Kobayashi et al., 1980). The advantage of this model in comparison with the *in vitro* and subcutaneous models lies in more authentic simulation of the actual conditions of malignant processes in the brain (Dong et al., 1994; Fidler et al., 1994; Killion et al., 1998). On the other hand, longitudinal monitoring of the tumour growth in an orthotopic model is a highly laborious and time-consuming task requiring a large number of experimental animals to be killed. To resolve this obstacle, imaging systems such as magnetic resonance imaging (MRI), positron emission tomography, bioluminescence imaging (BLI) and fluorescence imaging (FLI) have been put into practice for small animals. Compared to the expensive and low-throughput tomographic systems (Mook et al., 2008), the optical imaging systems based on light detection (i.e. BLI, FLI) have the advantage of low costs and easy equipment handling. Although two-dimensional information provided by these methods may bias precise volumetric estimations, several studies demonstrated high correlation of MRI and BLI results, and thus BLI is often used for brain tumour growth estimation (Szentirmai et al., 2006; Dinca et al., 2007; Hashizume et al., 2010). In contrast to that, the suitability of FLI for this purpose has not been validated, probably also because of the absence of an appropriate fluorescence reporter. The situation could, however, change with the introduction of a new category of red-shifted fluorescent proteins (Hoffman, 2008). Their emission wavelength beyond 600 nm dramatically decreases light absorption and scattering by the surrounding tissues, while their excitation wave-

Received September 29, 2011. Accepted January 12, 2012.

This work was supported by Research project MSM 0021620808 of the Czech Ministry of Education, Youth and Sports, grant No. 20410 of the Grant Agency of Charles University in Prague and SVV-2011-262513.

Corresponding author: Aleksi Šedo, Laboratory of Cancer Cell Biology of the Institute of Biochemistry and Experimental Oncology of the First Faculty of Medicine, Charles University in Prague, U Nemocnice 5, 128 53 Prague 2, Czech Republic. e-mail: aleksi@cesnet.cz

Abbreviations: BLI – bioluminescence imaging, DMEM – Dulbecco's Modified Eagle's Medium, FBS – foetal bovine serum, FLI – fluorescence imaging, MRI – magnetic resonance imaging.

length of about 590 nm produces less tissue autofluorescence (Troy et al., 2004; Tung et al., 2004). This improves their detectability by at least two orders of magnitude compared to the so far "gold standard" green fluorescent protein (Shcherbo et al., 2007, 2009; Deliolanis et al., 2008). Despite these promising characteristics of the red-shifted fluorescent proteins, there are no studies to confirm the correlation between the macroscopic FLI results and morphometric quantification of the brain tumour size.

The purpose of our study was to assess the reliability of tumour volume estimation by FLI in the epi-illumination mode for the *in vivo* studies of molecules and interventions affecting gliomagenesis. Our experiments using orthotopically implanted glioma xenografts transfected with red-shifted fluorescent protein mKate2 as a reporter and inducibly expressing growth-suppressing cell surface protease dipeptidyl peptidase-IV (DPP-IV, CD26) (Busek et al., 2008) demonstrate the limitations of the method.

Material and Methods

Cell culture

Human glioma cell line U373MG (originally derived from WHO grade III glioma) was obtained from the American Type Culture Collection (Rockville, MD). Cells were grown under standard cell culture conditions at 37 °C in Dulbecco's Modified Eagle's Medium (DMEM, Sigma-Aldrich Chemie, Steinheim, Germany) supplemented with 10% foetal bovine serum (FBS, Sigma-Aldrich Chemie), under a humidified (> 90 %) atmosphere of 5 % CO_2/95 % air.

Generation of transfected glioma cells

U373MG cells inducibly expressing the full-length human DPP-IV (Tet-On Advanced Inducible Gene Expression System, Clontech, Mountain View, CA*)* were transfected with the pcDNA4 vector (Invitrogen, Paisley, UK) containing the full-length cDNA of mKate2 (Evrogen, Moscow, RU) using Lipofectamine™ 2000 (Invitrogen) according to the manufacturer's instructions. Stable clones were selected after 6–8 weeks in complete medium containing 400 μg/ml Zeocin (Invitrogen).

Orthotopic xenotransplantation model

The experimental use of animals was approved by The Commission for Animal Welfare of the First Faculty of Medicine of Charles University in Prague and the Ministry of Education, Youth and Sports according to animal protection laws. Twenty adult male mice NOD.129S7(B6)-Rag1tm1Mom/J (The Jackson Laboratory, Bar Harbor, ME) weighing approximately 25 g were used in the experiment. All animals were anaesthetized prior to surgery with an intramuscular injection of Ketamine (100 mg/kg) and Xylazine (20 mg/kg). The operating area was depilated, disinfected and a 5 mm midsagittal incision was performed. The animal's head was fitted into the mouse adapter of a stereotaxic device (Stoelting, Wood Dale, IL) and a 0.4 mm borehole was drilled in the skull at a position 1.2 mm anterior from the bregma, 2.5 mm sagittal from the middle line. The total volume of 6 μl of cell suspension (200 000 cells/μl in DMEM, Sigma-Aldrich Chemie) was injected with a Hamilton syringe.

To limit the back flow along the needle track, the needle tip was initially sunk to a depth of 3.5 mm and then withdrawn 1 mm to a final depth of 2.5 mm. The injection time was set at 5 min. The needle was subsequently left in place for another 3 min after which it was slowly withdrawn. Immediately after removing the needle, the skull trephination was sealed with bone wax and the skin incision was closed with two surgical stitches. The animals were placed into heated cages until they awoke from anaesthesia. The experimental group of animals (N = 11) received doxycycline hyclate (Sigma-Aldrich Chemie) in drinking water (2 mg/ml) ad libitum during the 6-week period of tumour growth in order to induce DPP-IV expression in the xenografted glioma cells. The control group of animals (N = 9) received drinking water without doxycycline.

Fluorescence imaging

For animal imaging, an iBox® Scientia Small Animal Imaging System, (UVP, Upland, CA) coupled with a BioChemi HR 400 CCD camera (UVP) was used. The system in epi-illumination mode was equipped with a 150W halogen bulb and 533–587 nm excitation filter. A 607–682 nm emission filter was placed in front of the camera lens. The distance of the animal from the camera lens was 25 cm. All animals were scanned (exposure time 90 s) weekly during the 6-week period after implantation, all animal manipulations were done under anaesthesia; the scanned area was depilated prior to every imaging session. After the last imaging session, mice were sacrificed, the brain was removed from the skull within 5 min since the sacrifice and immediately placed into the imaging system at the identical position the live animal was previously scanned. In order to avoid oversaturation of the camera chip, the exposure time was reduced from 90 s to 10 s. Other settings of the system were the same as at the previous *in vivo* scannings. The brains were subsequently processed for morphometric determination of tumour volume as detailed bellow. Analysis of the scans was performed in the ImageJ software (National Institute of Health, USA). The means of fluorescence intensities of the arbitrary unit area were used for statistical evaluation.

Morphometric quantification of tumour volume

Forty-three days after cell implantation, all animals were killed under deep anaesthesia, the brains were removed from the skull, embedded in Jung Tissue Freezing Medium (Leica Microsystems, Nussloch, Germany) and frozen at a temperature of –70 °C. Serial frozen coronal sections 25 μm thick were cut using a cryotome (Bright Instruments, Huntingdon, UK) at a temperature

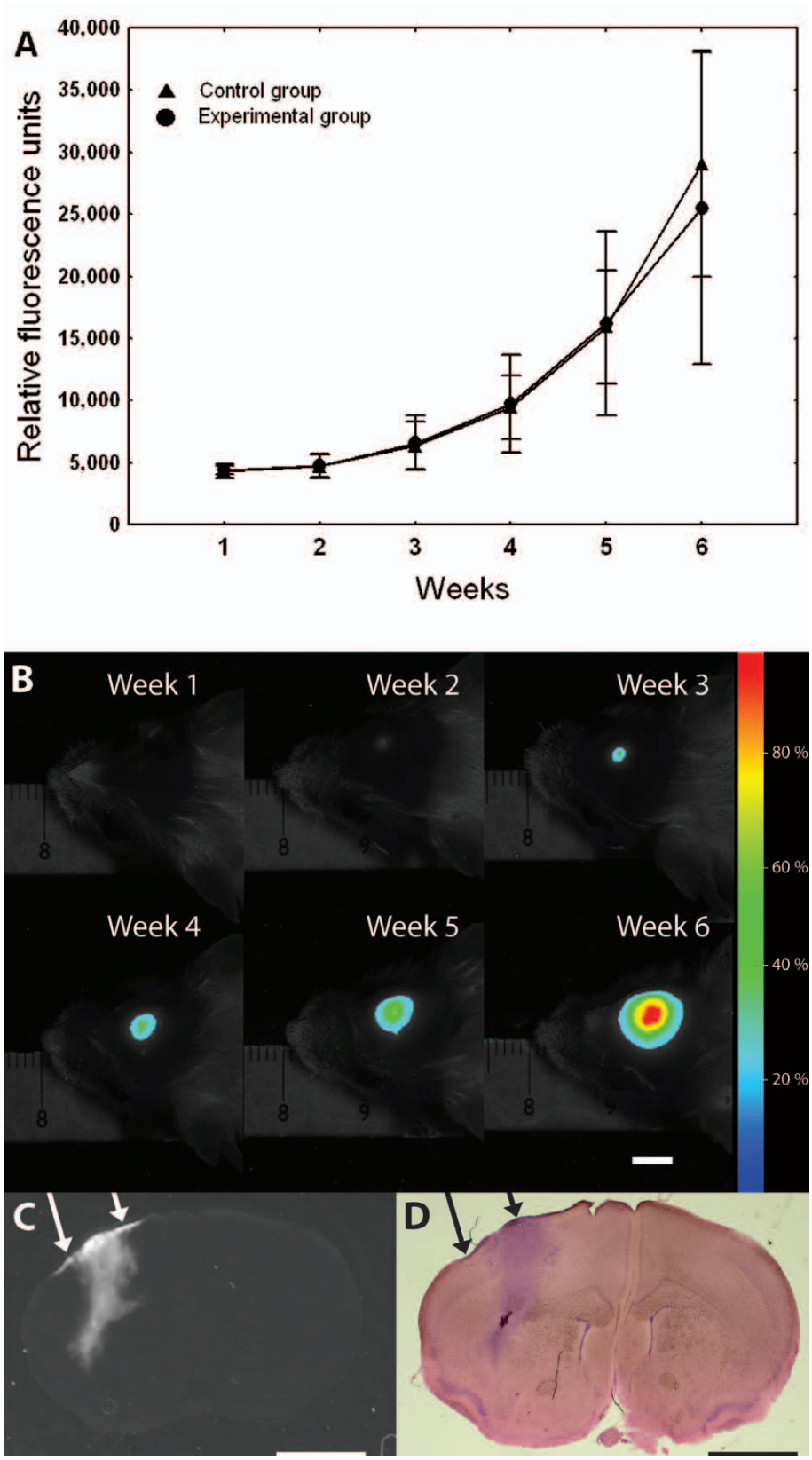

Fig. 1. Intracranial tumour growth assessed by *in vivo* epi-illumination fluorescence imaging and demonstration of tumour mass distribution in the brain section.
(A) Intravitally measured fluorescence in the control (N = 9) and experimental (N = 11) group during the 6-week period after the orthotopic implantation of glioma U373MG cells expressing the mKate2 protein. Data presented as mean ± S.D. (B) Scan of one representative animal. Exposure time, 90 s; scale bar, 5 mm. (C) Distribution of the tumour mass in the brain section visualized by fluorescence imaging and (D) by haematoxylin-eosin staining. The extracerebral portion of the tumour is indicated with arrows. Scale bars, 2 mm.

of –20 °C. Every fifth section was dyed with haematoxylin and eosin (Sigma-Aldrich Chemie) and digitized. Quantification of the tumour size was done using the Cavalieri's method for unbiased volume estimation (Mayhew and Olsen, 1991).

Assessment of the relative attenuation of fluorescence signal in the brain tissue

To assess the influence of the mass of surrounding brain tissue on the fluorescence signal detection, a fluorescent xenograft was simulated with a drop of 5 µl of Matrigel Matrix™ (BD Biosciences, Bedford, MA) containing 10^6 U373MG cells expressing mKate2 on the surface of a 3 mm thick coronal section of brain tissue. The gelatinous fluorescent bolus was scanned with a long exposure time (30 s) to achieve almost saturating pixel intensities. The scanning was subsequently performed with identical settings of the imaging system after covering the bolus with 1 mm thick brain tissue sections. This procedure was repeated until the bolus was covered with a total of 3 mm of brain tissue.

Results and Discussion

We observed an increasing fluorescence signal in both the control and experimental group over the six-week period after xenograft implantation (Fig. 1A, B). There was no statistically significant difference between the fluorescence intensities in the experimental group and the control group (Fig. 1A) at any time point during the study. In stark contrast with this, tumour volume determined morphometrically post mortem (week 6) was significantly different between the two groups (Fig. 2A). The *in vivo* fluorescence imaging data at week 6 showed no significant correlation (r = 0.26; P = 0.26; N = 20) with the morphometrically determined tumour volumes (Fig. 3A).

In addition to the intracranial tumour mass, we observed extracerebral growth of the tumours through meninges into the adjacent bone in all animals (Fig. 1C, D).

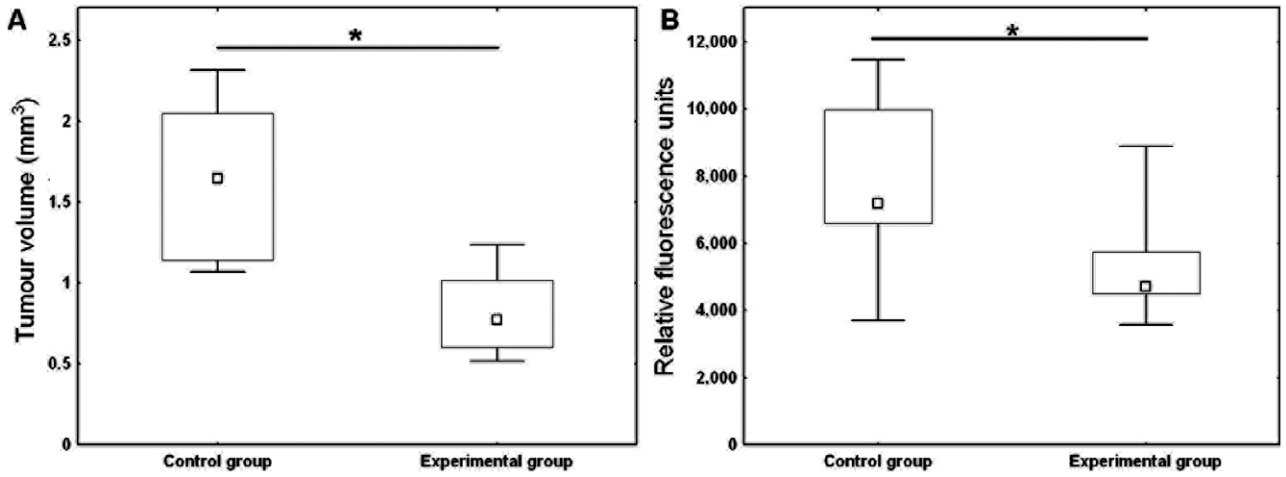

Fig. 2. Comparison of tumour size estimated morphometrically (A) and by the FLI in brains removed from the skull (B) at week 6.
Control group (N = 9), experimental group (N = 11). Squares: medians; boxes: middle 25–75 % of measured values; bars: minimal and maximal values; * P < 0.05, Mann-Whitney U test.

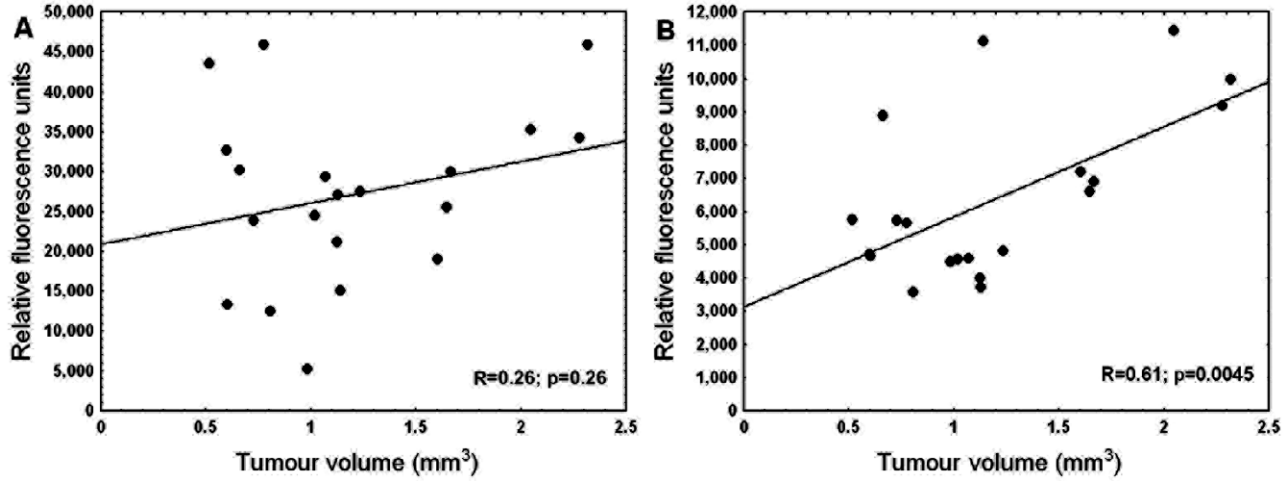

Fig. 3. Correlation of the morphometrically determined tumour volume and the corresponding fluorescence intensity measured *in vivo* (A) and in brains removed from the skull (B) at week 6. Spearman correlation, N = 20.

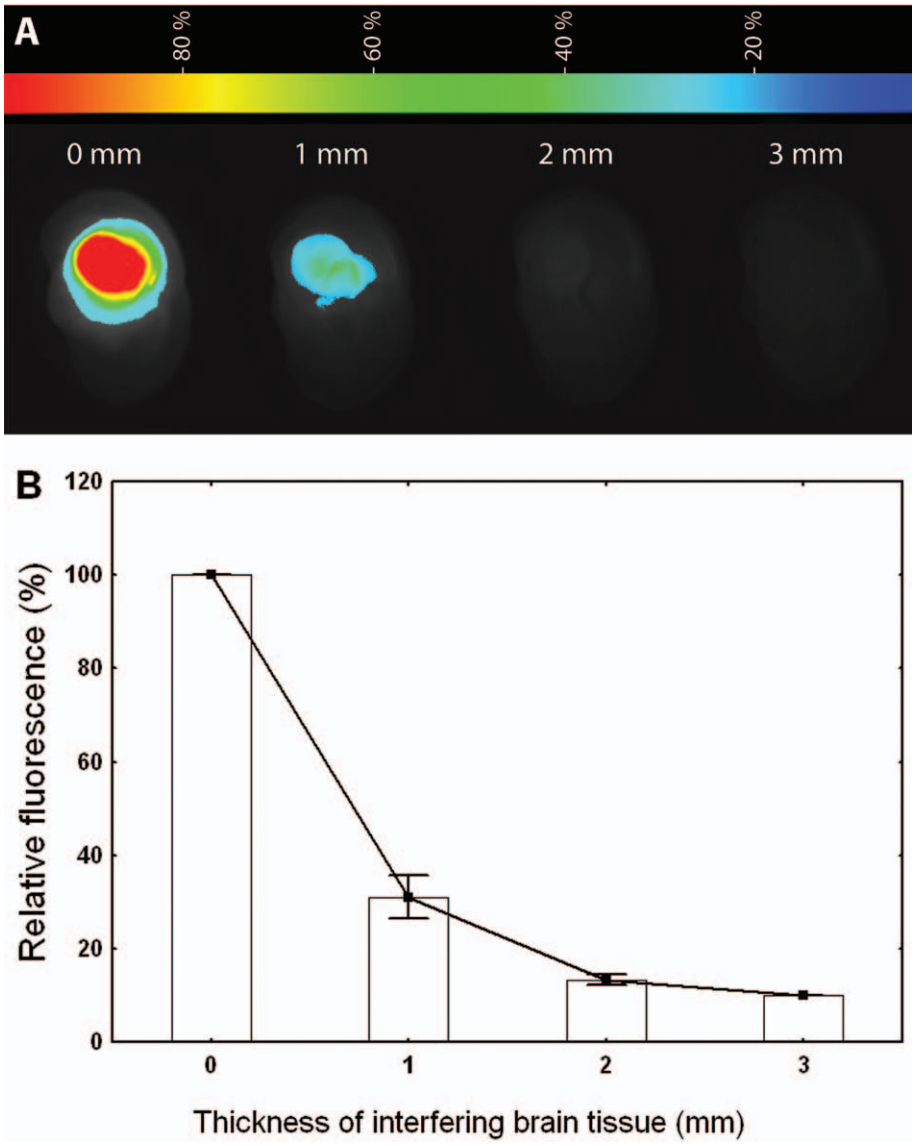

Fig. 4. Relative attenuation of the fluorescence signal by interfering brain tissue.
(A) Relative fluorescence of U373MG cells expressing the mKate2 protein, embedded in the Matrigel matrix, covered with brain tissue sections of the indicated thickness. (B) Relative attenuation of the fluorescence signal. Three independent experiments; data presented as mean ± S.D.

Removal of the brains from the skull and thus elimination of the signal from the overlying bone infiltrated by glioma cells led to the improvement of the correlation between the fluorescence signal and the morphometric data ($r = 0.61$; $P = 0.0045$; $N = 20$) (Fig. 3B). In addition, only the FLI data obtained from brains removed from the skull revealed the difference in tumour size between our two experimental groups (Fig. 2B).

In experiments simulating attenuation of the fluorescence signal in the brain tissue (see Material and Methods) the signal decreased by 65 % and 85 % when 1 mm and 2 mm of the brain tissue was superimposed over the fluorescent bolus (Fig. 4). Three mm of the superimposed brain tissue reduced the signal almost to the tissue autofluorescence values.

To the best of our knowledge, this is the first report that evaluates the use of macroscopic fluorescence imaging for the longitudinal monitoring of the growth of orthotopic gliomas in a mouse model. Our findings suggest that the estimation of the tumour growth based on the intensity of the fluorescence signal is strongly influenced by the spatial distribution of the tumour mass as well as by significant attenuation of the fluorescence signal by the surrounding brain tissue. The variable extracranial portions of the tumour caused by the migration of glioma cells into the subarochnoid or subdural space and eventually the adjacent bone, as well as superficially located intracerebral tumour masses may be responsible for a substantial part of the *in vivo* detected fluorescence signal, although they represent only a small fraction of the whole tumour mass. In our model, this is the most likely cause of the low correlation of the FLI data collected from living animals with the post-sacrifice morphometric volume estimation.

Extracerebral growth of the xenotransplanted brain tumours represents a frequently occurring phenomenon

(Antunes et al., 2000; Jost et al. 2007; Yang et al., 2007; Barth and Kaur, 2009), which can be partially limited by a deeper injection of a smaller volume of the cell suspension. However, the light emitted from a more deeply implanted tumour is more attenuated and scattered by the surrounding tissue, which causes a loss of imaging resolution (Ntziachristos, 2006). Reduction of the number of implanted cells leads to a reduction in the emitted signal, which, due to the interference from the tissue autofluorescence, does not provide a sufficiently strong signal to enable detection (Troy et al., 2004) at least in the early phases of tumour growth.

Together, the fluorescence signal emitted by glioma cells reflected not only the tumour mass, but also its spatial distribution and did not correlate with the tumour volume determined morphometrically. Macroscopic planar FLI in an epi-illumination mode and a conventional source of excitation light therefore appears to be more suitable for semi-quantitative observations and superficially located tumours rather than for precise volume estimation of the xenografts located deep within the brain.

Acknowledgement

Acquisition of the iBox was supported by the League Against Cancer Prague.

References

Antunes, L., Angioi-Duprez, K. S., Bracard, S. R., Klein-Monhoven, N. A., Le Faou, A. E., Duprez, A. M., Plénat, F. M. (2000) Analysis of tissue chimerism in nude mouse brain and abdominal xenograft models of human glioblastoma multiforme: what does it tell us about the models and about glioblastoma biology and therapy? *J. Histochem. Cytochem.* **48**, 847-858.

Barth, R. F., Kaur, B. (2009) Rat brain tumor models in experimental neuro-oncology: the C6, 9L, T9, RG2, F98, BT4C, RT-2 and CNS-1 gliomas. *J. Neurooncol.* 94, 299-312.

Busek, P., Stremenova, J., Sedo, A. (2008) Dipeptidyl peptidase-IV enzymatic activity bearing molecules in human brain tumors – good or evil? *Front. Biosci.* **13**, 2319-2326.

Deliolanis, N. C., Kasmieh, R., Würdinger, T., Tannous, B. A., Shah, K., Ntziachristos, V. (2008) Performance of the red-shifted fluorescent proteins in deep tissue molecular imaging applications. *J. Biomed. Opt.* **13**, 044008.

Dinca, E. B., Sarkaria, J. N., Schroeder, M. A., Carlson, B. L., Voicu, R., Gupta, N., Berger, M. S., James, C.D. (2007) Bioluminescence monitoring of intracranial glioblastoma xenograft: response to primary and salvage temozolomide therapy. *J. Neurosurg.* **107**, 610-616.

Dong, Z., Radinsky, R., Fan, D., Tsan, R., Bucana, C. D., Wilmanns, C., Fidler, I. J. (1994) Organ-specific modulation of steady-state mdr gene expression and drug resistance in murine colon cancer models. *J. Natl. Cancer Inst.* **86**, 913-920.

Fidler, I. J., Wilmanns, C., Staroselsky, A., Radinsky, R., Dong, Z., Fan, D. (1994) Modulation of tumor cell response to chemotherapy by the organ environment. *Cancer Metastasis Rev.* **13**, 209-222.

Hashizume, R., Ozawa, T., Dinca, E. B., Banerjee, A., Prados, M. D., James, C. D., Gupta, N. (2010) A human brainstem glioma xenograft model enabled for bioluminescence imaging. *J. Neurooncol.* **96**, 151-159.

Hoffman, R. M. (2008) A better fluorescent protein for whole-body imaging. *Trends Biotechnol.* **26**, 1-4.

Jost, S. C., Wanebo, J. E., Song, S. K., Chicoine, M. R., Rich, K. M., Woolsey, T. A., Lewis, J. S., Mach, R. H., Xu, J., Garbow, J. R. (2007) *In vivo* imaging in a murine model of glioblastoma. *Neurosurgery* **60**, 360-370; discussion 370-371.

Killion, J. J., Radinsky, R., Fidler, I. J. (1998) Orthotopic models are necessary to predict therapy of transplantable tumors in mice. *Cancer Metastasis Rev.* **17**, 279-284.

Kobayashi, N., Allen, N., Clendenon, N. R., Ko, L. W. (1980) An improved rat brain-tumor model. *J. Neurosurg.* **53**, 808-815.

Mayhew, T. M., Olsen, D. R. (1991) Magnetic resonance imaging (MRI) and model-free estimates of brain volume determined using the Cavalieri principle. *J. Anat.* **178**, 133-144.

Mook, O. R., Jonker, A., Strang, A. C., Veltien, A., Gambarota, G., Frederiks, W. M., Heerschap, A., Van Noorden, C. J. F. (2008) Noninvasive magnetic resonance imaging of the development of individual colon cancer tumors in rat liver. *BioTechniques* **44**, 529-535.

Ntziachristos V. (2006) Fluorescence molecular imaging. *Annu. Rev. Biomed. Eng.* **8**, 1-33.

Shcherbo, D., Merzlyak, E. M., Chepurnykh, T. V., Fradkov, A. F., Ermakova, G. V., Solovieva, E. A., Lukyanov, K. A., Bogdanova, E. A., Zaraisky, A. G., Lukyanov, S., Chudakov, D. M. (2007) Bright far-red fluorescent protein for whole-body imaging. *Nat. Methods* **4**, 741-746.

Shcherbo, D., Murphy, C. S., Ermakova, G. V., Solovieva, E. A., Chepurnykh, T. V., Shcheglov, A. S., Verkhusha, V. V., Pletnev, V. Z., Hazelwood, K. L., Roche, P. M., Lukyanov, S., Zaraisky, A. G., Davidson, M. W., Chudakov, D. M. (2009) Far-red fluorescent tags for protein imaging in living tissues. *Biochem. J.* **418**, 567-272.

Szentirmai, O., Baker, C. H., Lin, N., Szucs, S., Takahashi, M., Kiryu, S., Kung, A. L., Mulligan, R.C., Carter, B. S. (2006) Noninvasive bioluminescence imaging of luciferase expressing intracranial U87 xenografts: Correlation with magnetic resonance imaging determined tumor volume and longitudinal use in assessing tumor growth and antiangiogenic treatment effect. *Neurosurgery* **58**, 365-372.

Troy, T., Jekic-McMullen, D., Sambucetti, L., Rice, B. (2004) Quantitative comparison of the sensitivity of detection of fluorescent and bioluminescent reporters in animal models. *Mol. Imaging* **3**, 9-23.

Tung, C. H., Zeng, Q., Shah, K., Kim, D. E., Schellingerhout, D., Weissleder, R. (2004) *In vivo* imaging of β-galactosidase activity using far red fluorescent switch. *Cancer Res.* **64**, 1579-1583.

Yang, H., Chopp, M., Zhang, X., Jiang, F., Zhang, Z., Kalkanis, S., Schallert, T. (2007) Using behavioral measurement to assess tumor progression and functional outcome after antiangiogenic treatment in mouse glioma models. *Behav. Brain Res.* **182**, 42-50.